

Topological Phases Driven By Orbital Entanglement In Transition Metal Oxide Perovskite Interfaces

Impact 2024 meeting
Cargese, Corsica
Aug. 19-31, 2024



Mark Goerbig



Florian Simon

M. Gabay
Laboratoire de Physique des Solides
Université Paris-Saclay

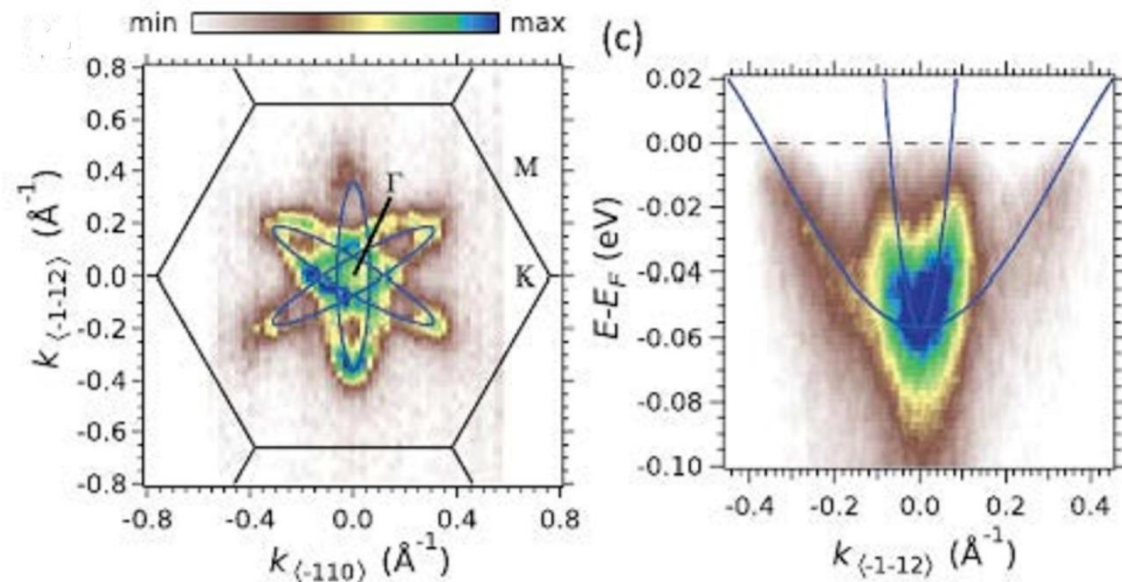
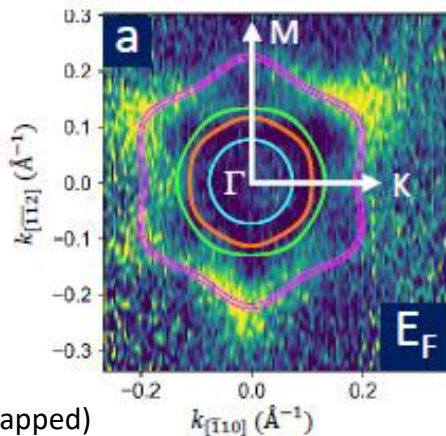


Acknowledgments:
M. Bibes, A. Caviglia, J-M Triscone



111-oriented surfaces or interfaces of transition metal oxide perovskites ABO_3

- ❖ Pure ABO_3 is insulating. Doping \rightarrow metallic state where carriers hop from B to B via O ; B (Ti, Ta..) , A (Ba, Sr, Ca, K,..)
- ❖ Generic band spectrum derived from t_{2g} orbitals.
- ❖ Experimental spectrum is well captured by a tight-binding modeling (+ Poisson Schroedinger)
- ❖ **111-orientation gives rise to geometric contributions which promote orbital- and spin- tronic transport and lead to a non standard superconducting regime**

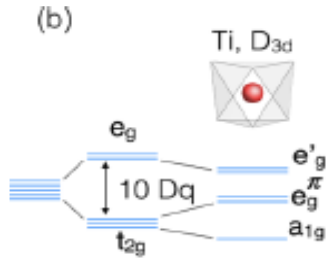


KTO 111 (Eu capped)

STO 111 (cleaved)

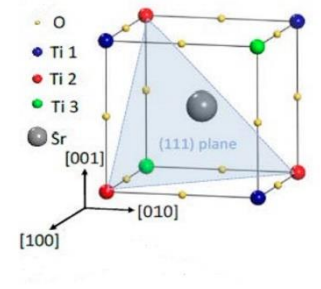
→ Modeling the electronic structure of 111-oriented 2DEG

○ Trigonal crystal field



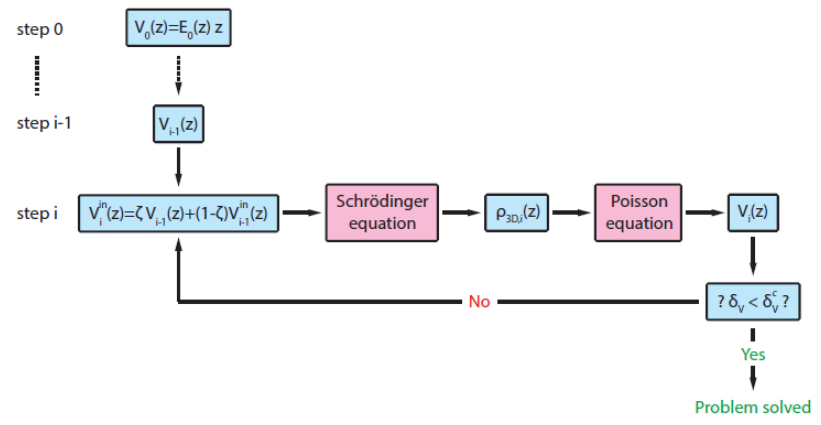
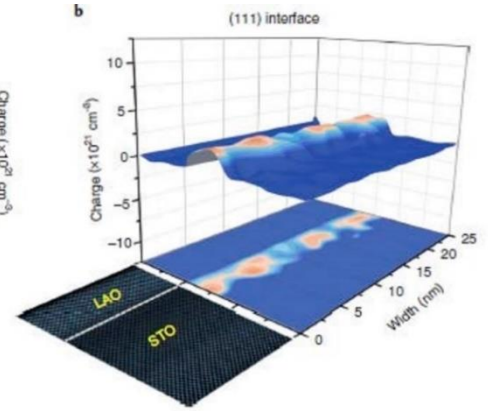
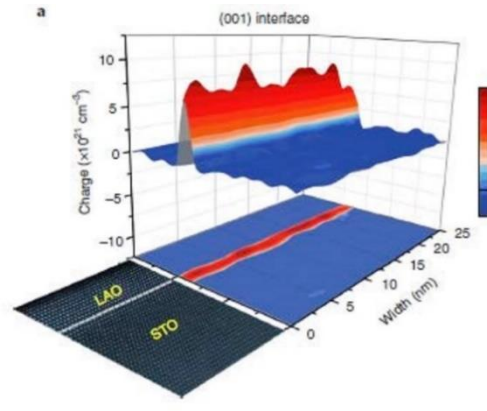
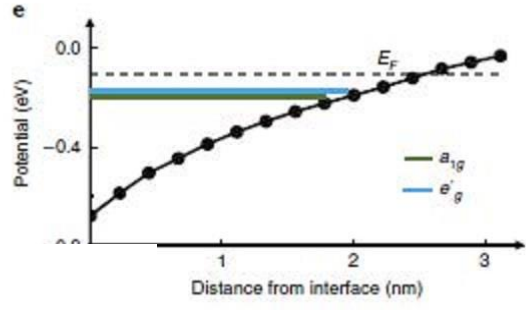
$3d = 10meV$ (LAO/STO)

Salluzzo et al. Phys Rev B 98 115 143 (2018)

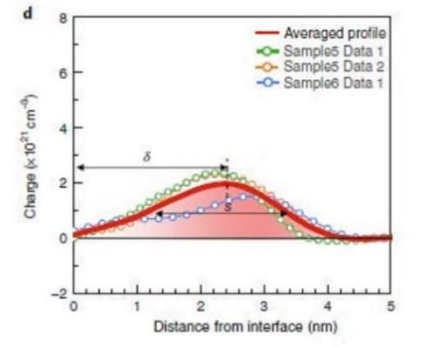
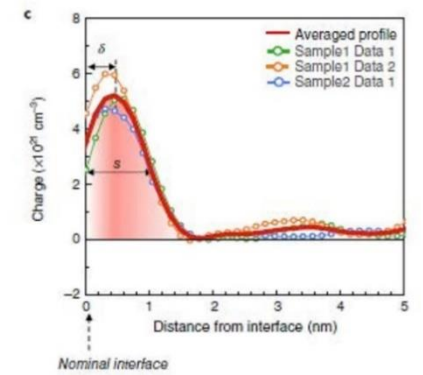


○ Confinement near surface/interface (same for all orbitals) $V \sim 100meV$

K. Song et al. Nat. Nanotechnology 13, 198 (2018)

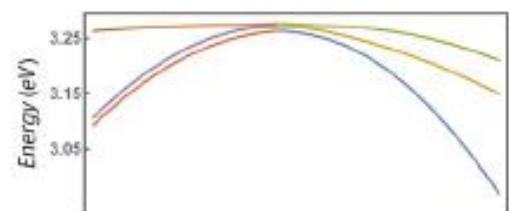
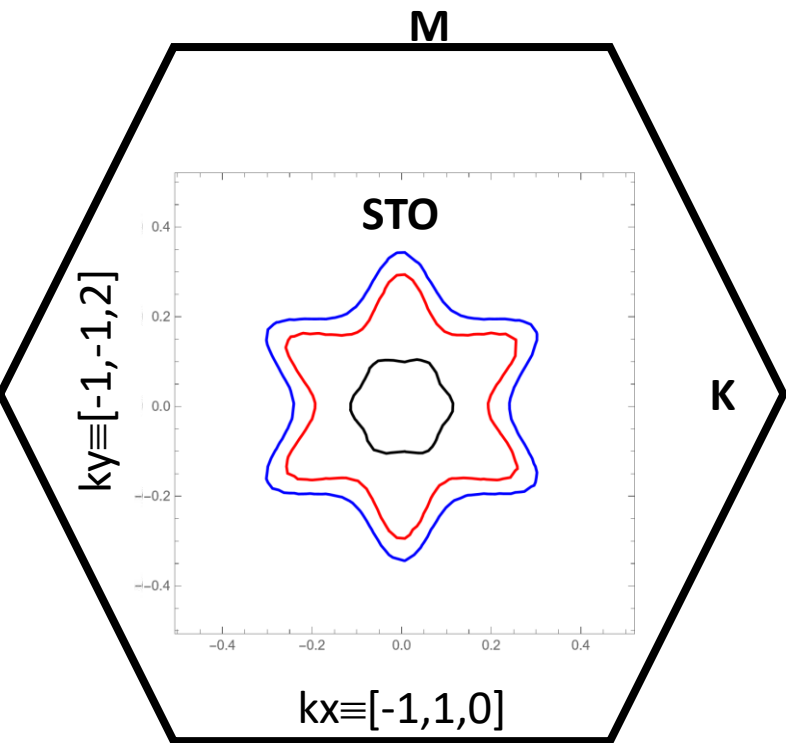
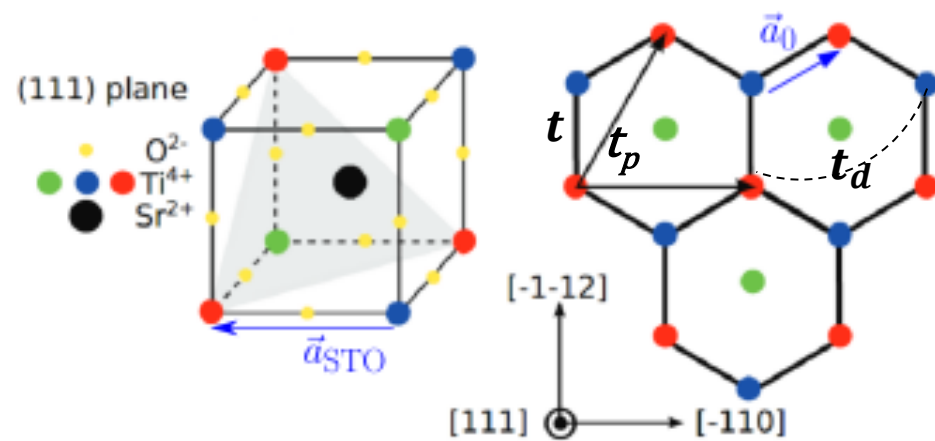


+ Hubbard U

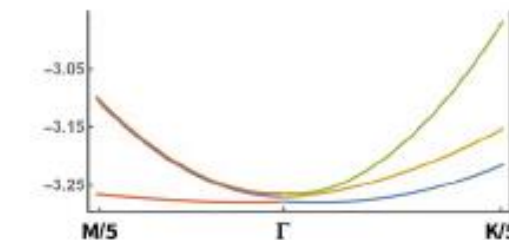


- 2D Kinetic energy (nearest neighbor hops are between layers)

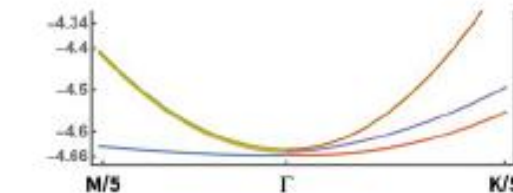
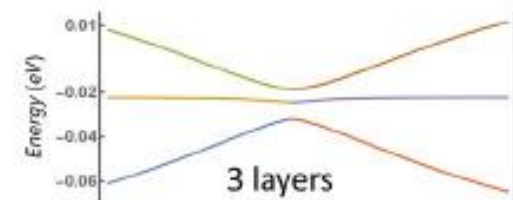
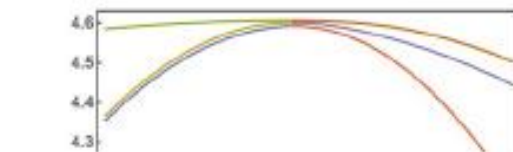
Hopping amplitudes $t=1.6$ eV, $t_d=70$ meV (STO)
 $t=1.8$ eV, $t_d=100$ meV, $t_p=140$ meV (KTO)



Antibonding bands

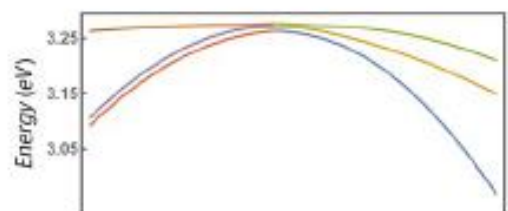
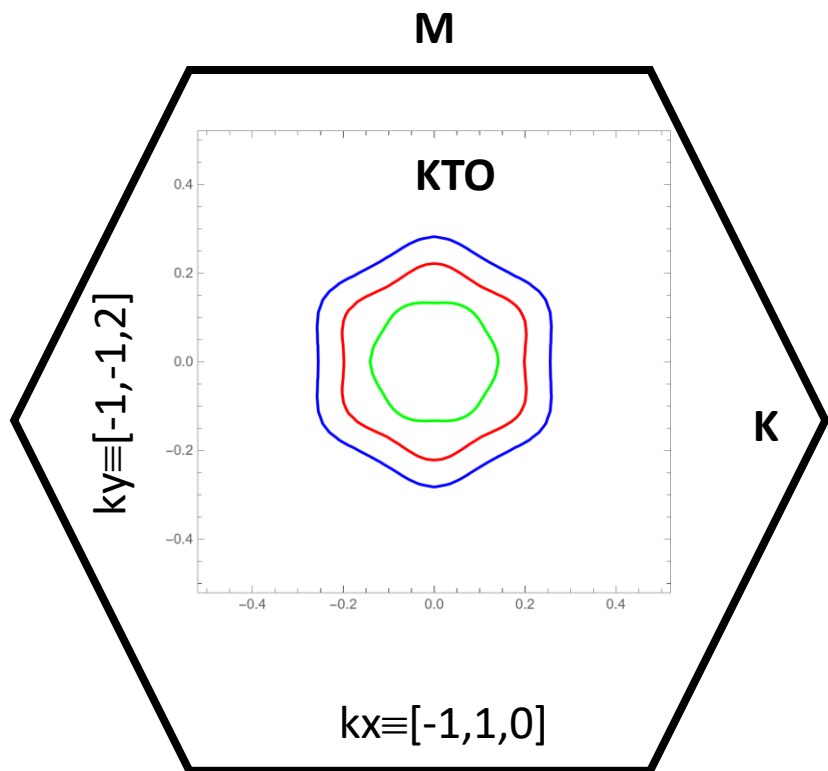
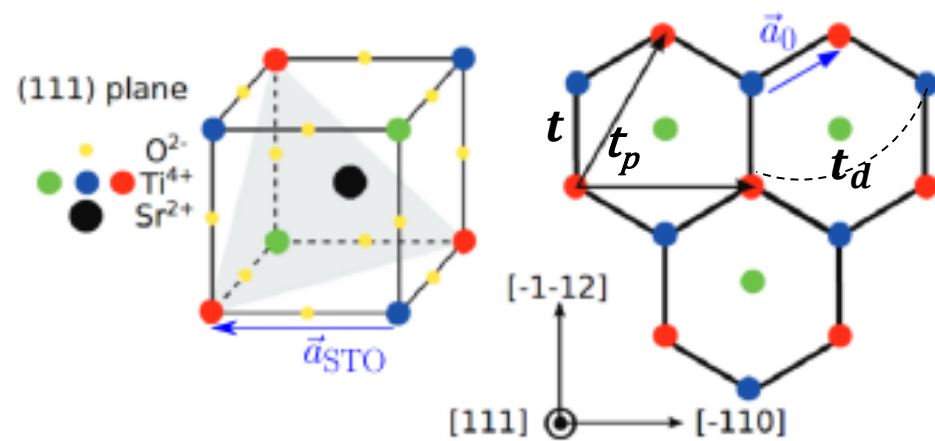


Non-bonding bands



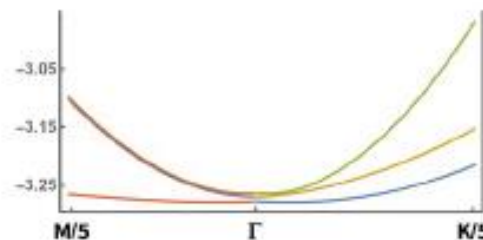
- 2D Kinetic energy (nearest neighbor hops are between layers)

Hopping amplitudes $t=1.6$ eV, $t_d=70$ meV (STO)
 $t=1.8$ eV, $t_d=100$ meV, $t_p=140$ meV (KTO)



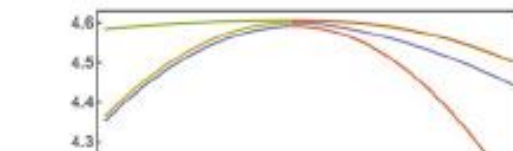
Antibonding bands

2 layers

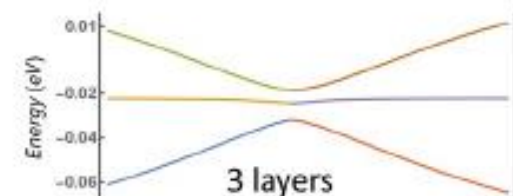


Bonding bands

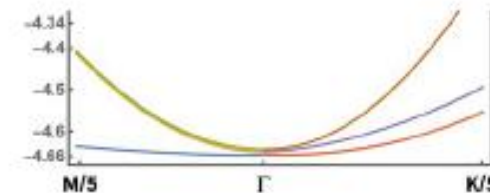
Gap 8 meV at Γ between lowest 2 bands



Non-bonding bands



3 layers

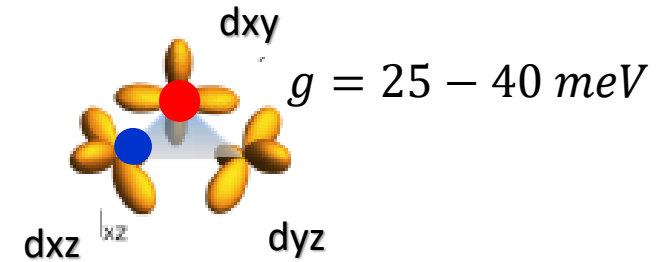
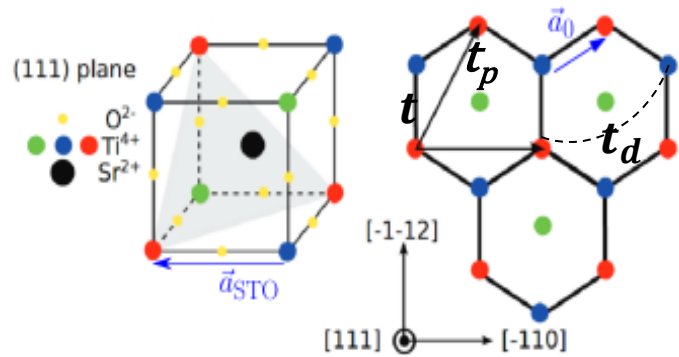


- Atomic spin-orbit

$$E_{SO} \sim 25 \text{ meV (STO)}, E_{SO} \sim 400 \text{ meV (KTO)}$$

- Orbital mixing (at the surface/interface, bond distortions → the orbital character can change after a hop)

Symmetries : rotation about (111) diagonal of cube and mirror plane [1,1,1]-[-1,-1,2] →

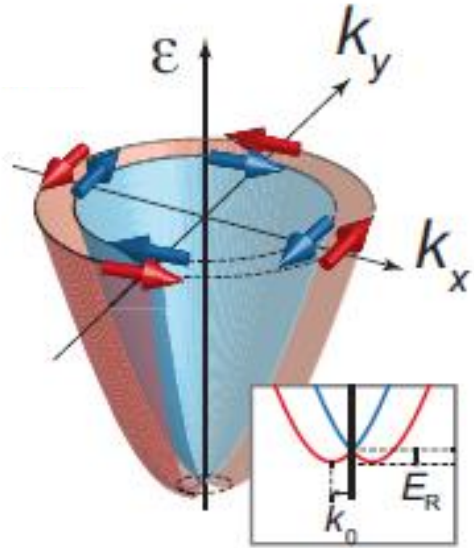


$$H_{OM} = \mathbf{d} \cdot \mathbf{L}$$

L=1 angular momentum operator in the t_{2g} Hilbert space (Gell-Mann matrices)

$$g \left(\sin\left(\frac{\sqrt{3}}{2} k_x a_0 - \frac{3}{2} k_y a_0\right), \sin\left(\frac{\sqrt{3}}{2} k_x a_0 + \frac{3}{2} k_y a_0\right), -\sin(\sqrt{3} k_x a_0) \right)$$

In the low energy (small k) limit, $H_{OM} = (\mathbf{g} a_0) \mathbf{L} \cdot (\mathbf{k} \times \mathbf{u}_z)$ Orbital Rashba Hamiltonian; cf spin Rashba $\sim \alpha_R \boldsymbol{\sigma} \cdot (\mathbf{k} \times \mathbf{u}_z)$



Y. A. Bychkov and E. I. Rashba, *JETP Lett.* **39**, 78–81 (1984)

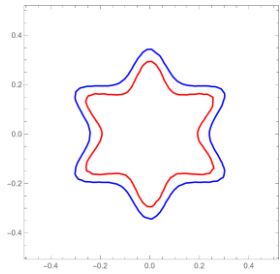
- Rotational symmetry breaking about (111) axis at low T (STO)

E. Lesne et al. *Nat. Materials* 22, 576 (2023) M.T Mercaldo et al. *NPJ Quantum Materials* 8, art #12 (2023)

→ Orbital winding

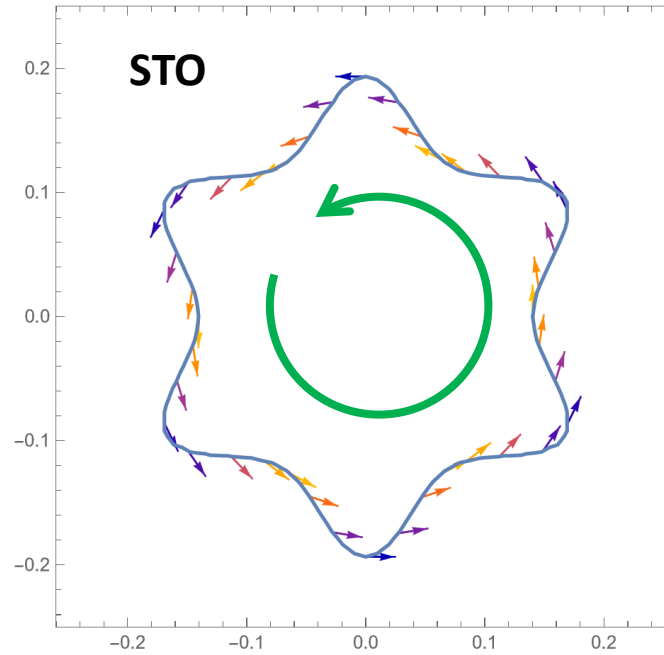
Berry contributions are driven by orbital textures : $E_{SO}=0$

In-plane (L_x, L_y) textures (lowest 2 bands)

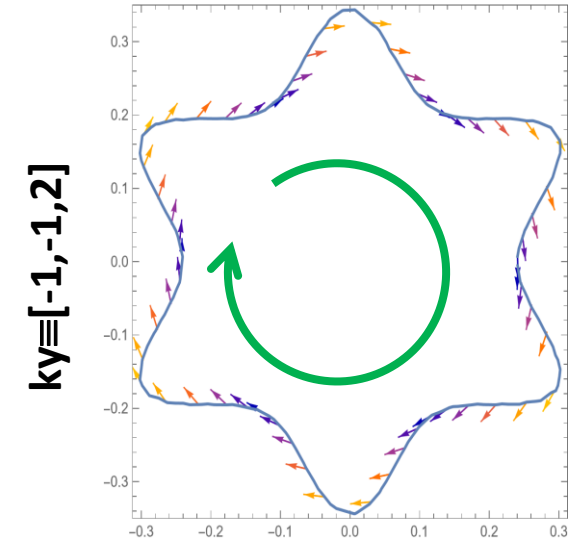


$k_y \equiv [-1, -1, 2]$

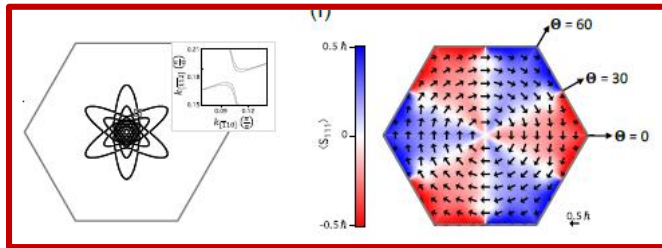
$k_x \equiv [-1, 1, 0]$



$k_x \equiv [-1, 1, 0]$

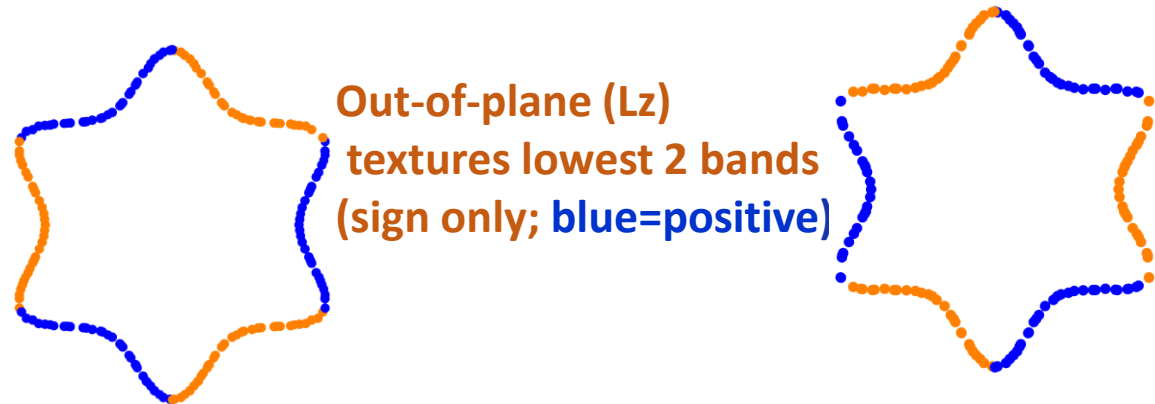


$k_y \equiv [-1, -1, 2]$



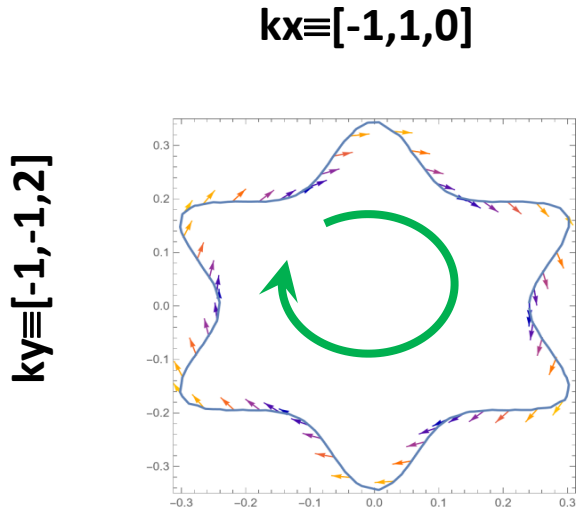
Arpes **STO111** Pan He et al.
Phys. Rev. Lett 2018

Out-of-plane (L_z)
textures lowest 2 bands
(sign only; blue=positive)

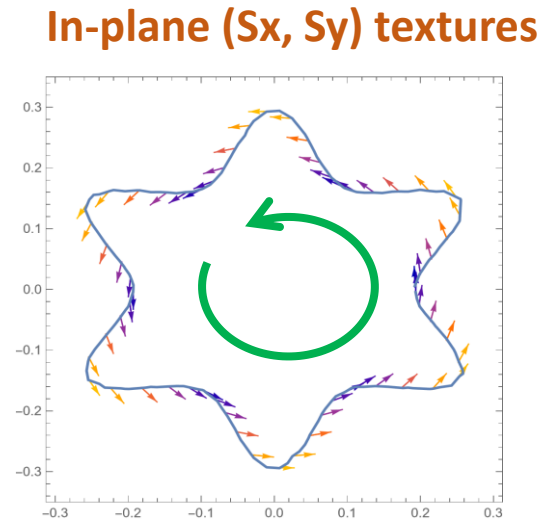


→ Spin winding

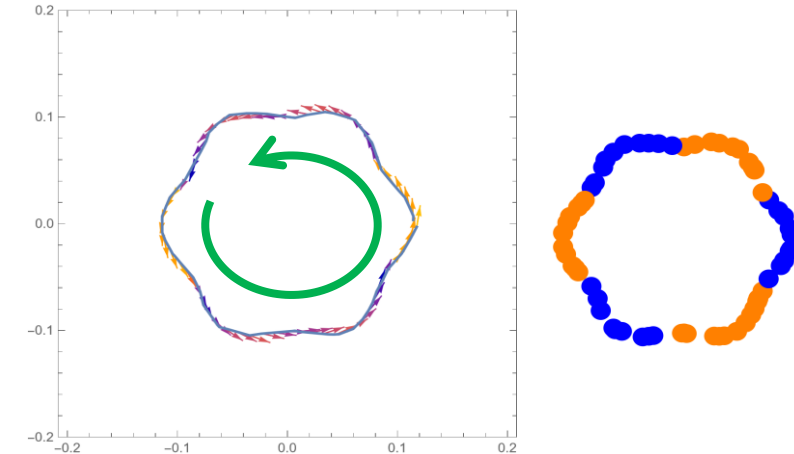
Spin effect : spin textures and additional BC contributions → We “turn spin-orbit on” ($E_{SO} \neq 0$)



“Blue band”

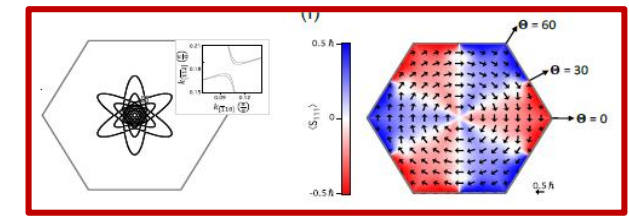
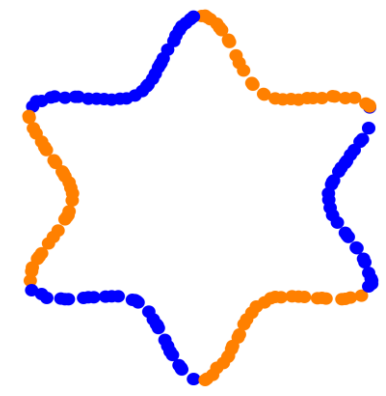
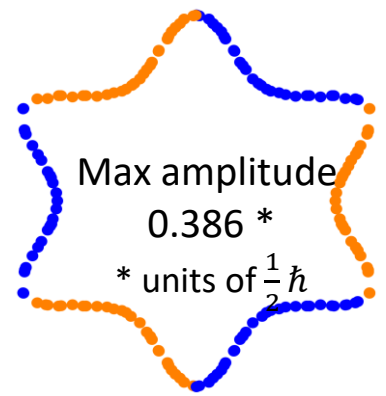


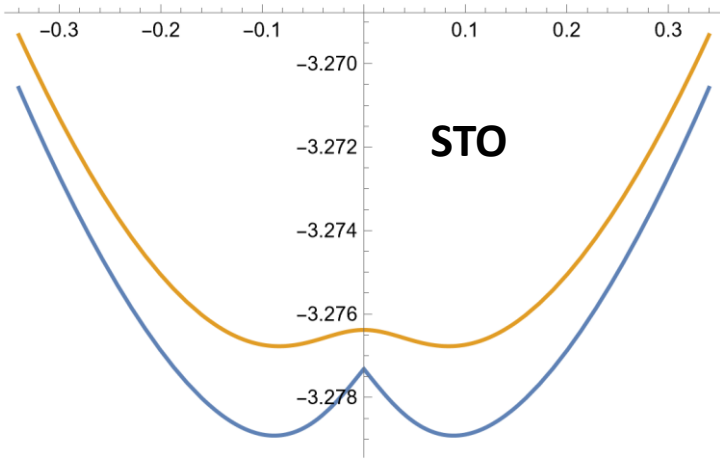
“Red band”



Third band

Out-of-plane (S_z) textures (sign only; blue=positive)





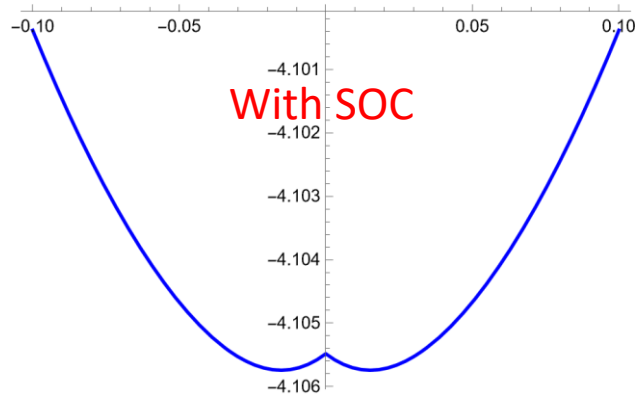
$$k_R a_0 = \frac{t_R}{t} \rightarrow \Delta k_R a_0 = \frac{t_{RST}}{t} \quad t_{RST} : \text{spin texture part of } t_R$$

$$t_{RST} = 4.8 \text{ meV}$$

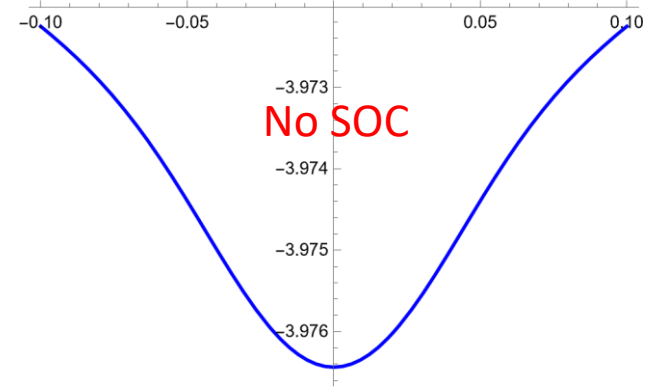
Dispersion along the (-1,-1,2) direction

- with orbital mixing and spin-orbit (blue)
- with orbital mixing but no spin-orbit (orange)

At Γ we get an estimate of the effective spin-orbit energy. $\beta_{SO} \sim 1 \text{ meV}$



KTO



At Γ we get an estimate of the effective spin-orbit energy. $\beta_{SO} \sim 129 \text{ meV}$

$$k_R a_0 = \frac{t_R}{t} \rightarrow \Delta k_R a_0 = \frac{t_{RST}}{t}$$

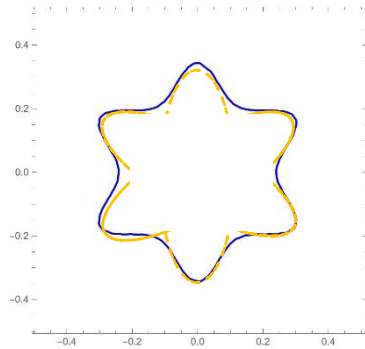
$$t_{RST} = 21 \text{ meV}$$

t_{RST} : spin texture part of t_R

→ Berry curvature (BC), Berry dipole (BCD)

Pure orbital contributions give rise to a BC near Γ → We “turn spin-orbit off” ($E_{SO} = 0$)

$$H_{TOT} = H_{KIN} + H_{TRIG} + H_{CONFIN} + H_{OM} \quad (6 \times 6)$$



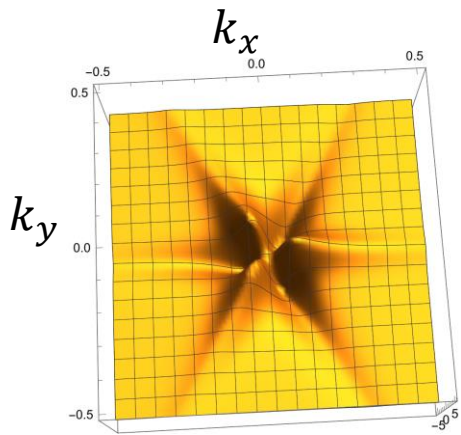
anisotropy of the
band structure

+ **mixing of bonding and antibonding
components of the eigenfunctions (e.g $\langle \text{bonding} | v | \text{antibonding} \rangle$).**

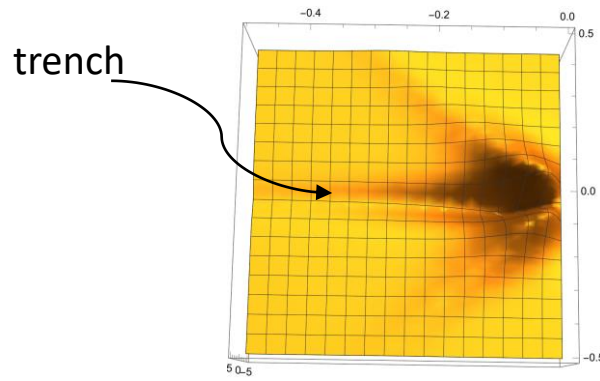
For $L=1$ one can generalize the expression found for 2-band case (A. Graf and F. Piechon Phys. Rev. B 104, 085114 (2021)). But for all practical purposes it is easier to use the generic form

$$\Omega_{\alpha}^z = -2 \operatorname{Im} \sum_{\beta \neq \alpha} \left[\frac{\langle u_{k\alpha} | \frac{\partial H_{TOT}}{\partial kx} | u_{k\beta} \rangle \langle u_{k\beta} | \frac{\partial H_{TOT}}{\partial ky} | u_{k\alpha} \rangle}{(E_{\alpha} - E_{\beta})^2} \right]$$

$|u_{k\lambda}\rangle$ (E_{λ}) eigen-vectors (values) of H_{TOT}

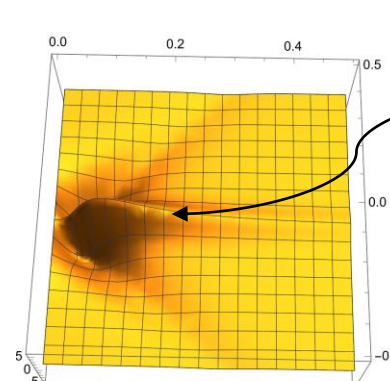


$\Omega^z(k_x, k_y)$



trench

$k_x \leq 0$



ridge

$k_x \geq 0$

Shows that the Berry curvature is even in k_y and odd in $k_x \rightarrow$ Berry curvature dipole

$$D_x = \frac{1}{(2\pi)^2} \int d_2k \frac{\partial \Omega^z}{\partial k_x} f_0 \quad f_0 \text{ Fermi factor;}$$

$D_x = 0.02$ (0.06) a_0 for STO (KTO). When filling such that higher levels (8meV higher) get populated, $D_x \nearrow 80$ then drops

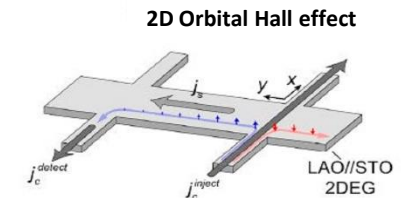
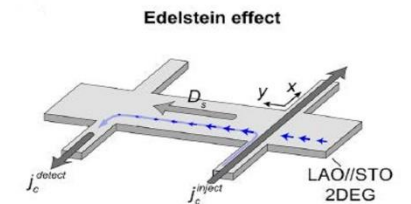
❑ Non linear second harmonic Hall current $\rightarrow \mathbf{j}_{2\omega} = \frac{1}{\hbar^2} \frac{e^3 \tau}{2(1+i\omega\tau)} \hat{z} \times \boldsymbol{\mathcal{E}}(\mathbf{D} \cdot \boldsymbol{\mathcal{E}}) \quad (\boldsymbol{\mathcal{E}} // \hat{x})$

Sodemann, Fu PRL 115, 216806 (2015), Lesne et al. (2023)

❑ Orbital Edelstein effect \rightarrow orbital moment accumulation (Kerr)

❑ Orbital Berry Hall current transverse to current flow $\rightarrow \sigma_{xy} \sim \sum_{\alpha} \iint \frac{d^2k}{(4\pi^2)} f_{0\alpha} \omega_{xy}^{\alpha z}$

$$\omega_{xy}^{\alpha z} = -2 \text{Im} \sum_{\beta \neq \alpha} \left[\frac{\langle u_{k\alpha} | \mathcal{J}_{xz} | u_{k\beta} \rangle \langle u_{k\beta} | \frac{\partial H_{TOT}}{\partial k_y} | u_{k\alpha} \rangle}{(E_{\alpha} - E_{\beta})^2} \right] \text{ where } \mathcal{J}_{xz} = \left\{ \frac{\partial H_{TOT}}{\partial k_x}, L_z \right\}$$



→ Quantum geometry and superconductivity

The quantum geometric tensor characterizes the k-space metric of the Hamiltonian eigenstates n .

$$Q_{\alpha\beta}^n = \left[\left\langle \frac{\partial n}{\partial k_\alpha} \middle| (1 - |n\rangle\langle n|) \middle| \frac{\partial n}{\partial k_\beta} \right\rangle \right] = g_{\alpha\beta}^n - \frac{i}{2} \Omega_{\alpha\beta}^n$$

$g_{\alpha\beta}^n$ is a real symmetric tensor (“distance” between quantum states in k-space) (*)

$\Omega_{\alpha\beta}^n$ is an antisymmetric tensor (Berry curvature in k-space)

* See Sala et al. arXiv:2407.06659

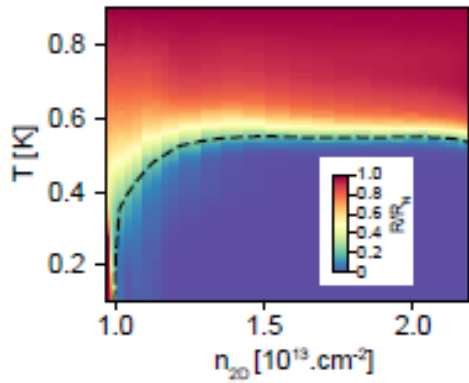
$\mathbf{j}(\mathbf{q}, \omega) = \mathbf{K}(\mathbf{q}, \omega)\mathbf{A}(\mathbf{q}, \omega)$; the superfluid weight $D \propto K(\mathbf{q} \rightarrow \mathbf{0}, \omega = 0)$

The superfluid weight $D = \frac{\hbar^2}{\mu_0 e^2} \frac{1}{\Lambda_{2D}}$ Λ_{2D} is the Pearl length. $D \propto$ superfluid density/m*

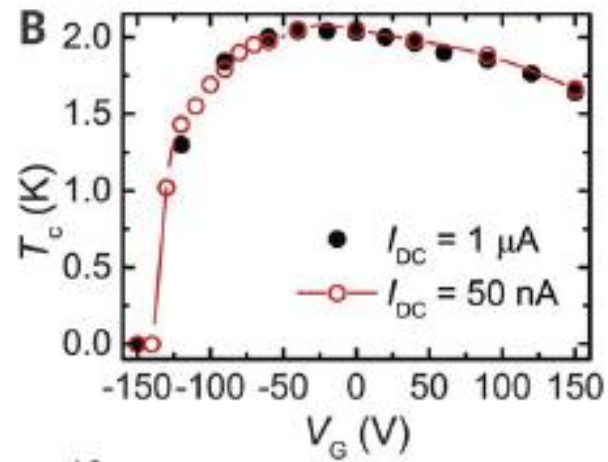
In 2D, for an isotropic case, $T_{BKT} = \frac{\pi}{8k_B} D(T_{BKT})$

$$D = D_{\text{conv}} + D_{\text{geom}} \rightarrow \propto \iint d_2 k f(k) g_{\alpha\beta}^n(k)$$

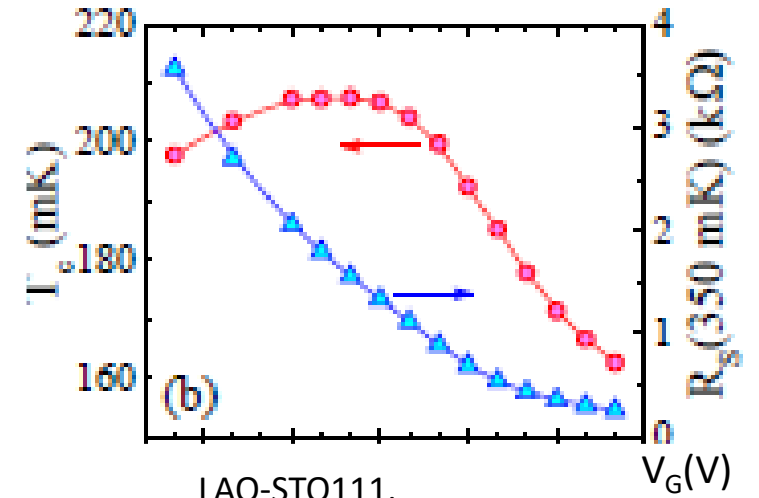
See e.g. Bernevig et al. *Nat. Rev. Phys.*, 528–542 (2022)



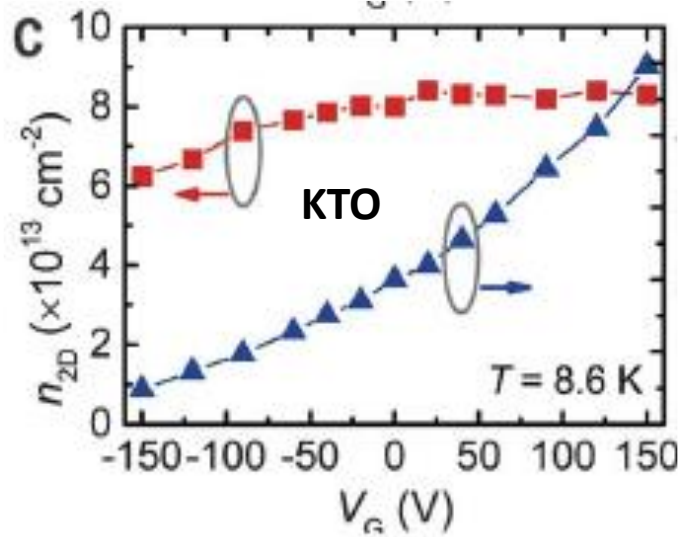
Superfluid density KTO111,
Mallik et al. Nat. Comm. 13, 4625 (2022)



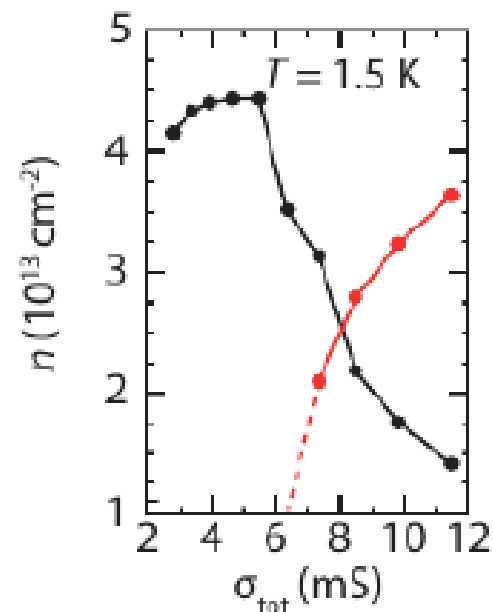
LAO-KTO111,
Chen et al. Science 372, 721 (2021)



LAO-STO111,
Rout et al. PRL 119, 237002 (2017)

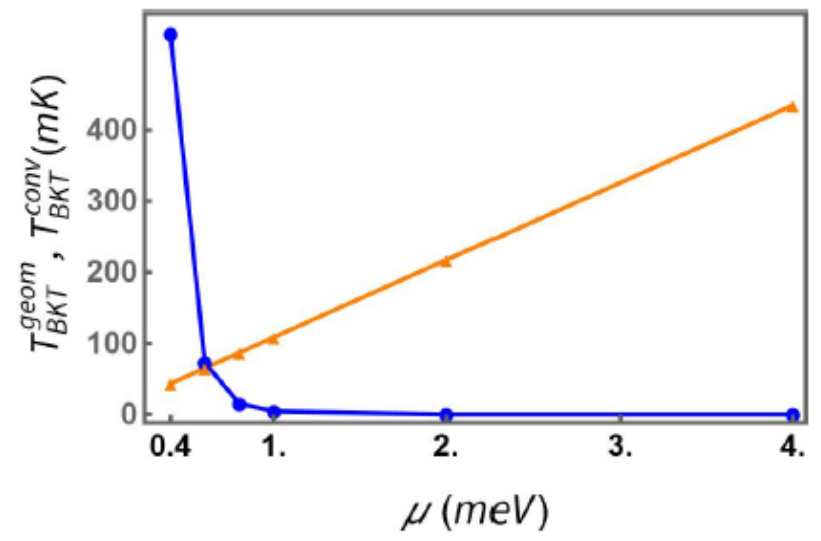
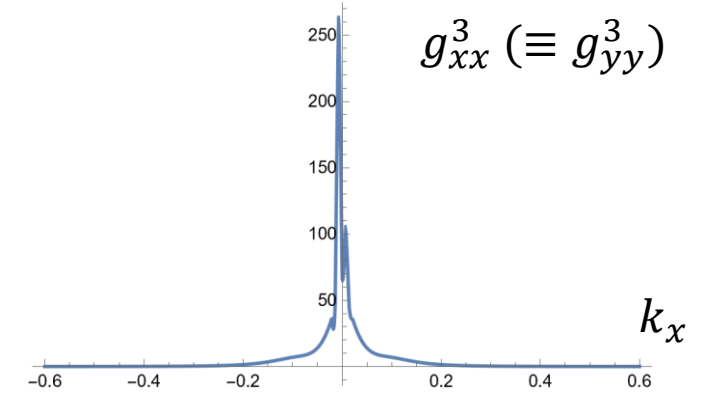
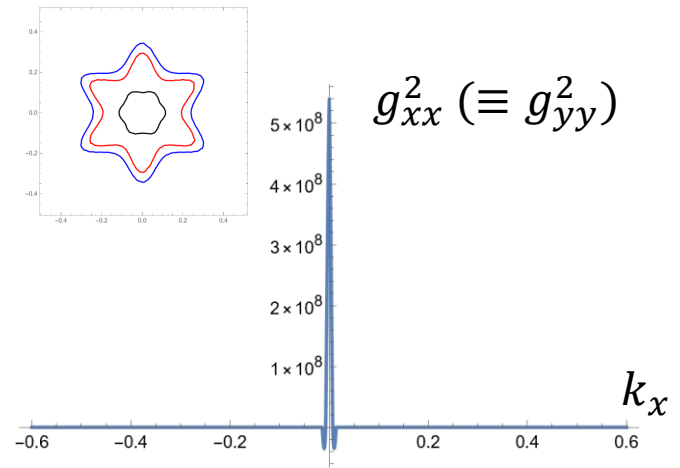
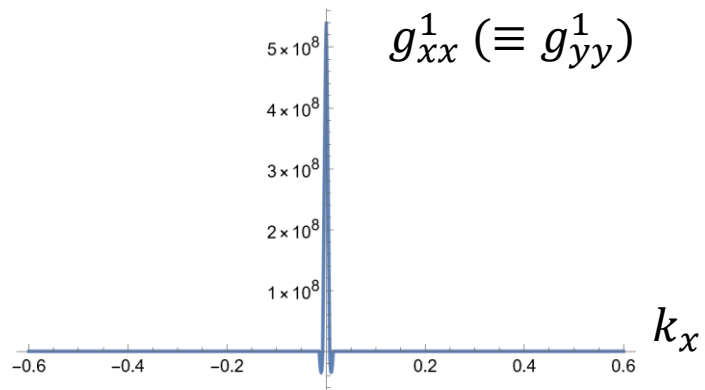


Chen et al., Science 372, 721-724 (2021)

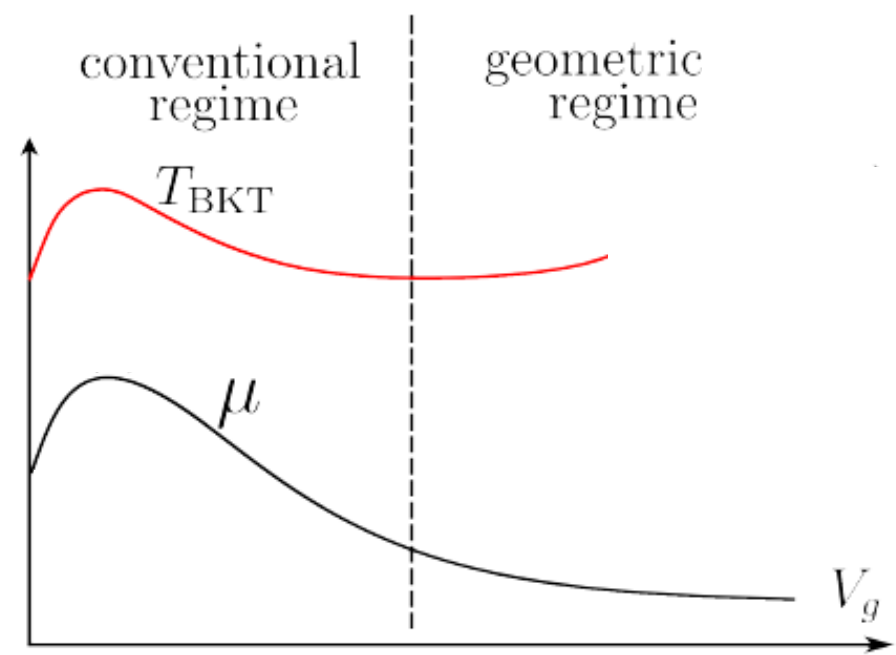


LAO/STO

M. Monteiro et al. PRB 99, 201102 (2019), U. Khanna et al. PRL 123, 036805 (2019)



F. Simon et al. [arXiv:2307.13993](https://arxiv.org/abs/2307.13993)



→ Symmetry of the superconducting gap

The prominent role played by the effective interfacial spin-orbit interaction (mediated by the orbital-mixing, OM) allows for the possibility of spin-triplet superconductivity.

$$H(k) = \sum (\varepsilon(k) - \mu) c_{k\sigma}^\dagger c_{k\sigma} + \frac{1}{2} \sum \Delta_{\sigma\sigma'}(k) c_{k\sigma}^\dagger c_{-k\sigma'}^\dagger + \frac{1}{2} \sum \Delta_{\sigma'\sigma}^* c_{-k\sigma'} c_{k\sigma} + \alpha \sum \mathbf{g}(k) \cdot \boldsymbol{\sigma}_{\sigma\sigma'} c_{k\sigma}^\dagger c_{k\sigma'}$$

$\varepsilon(k)$ dispersion of the energy bands of the tight-binding Hamiltonian *without* the “Rashba-spin” contribution due to the OM term.

$\alpha \mathbf{g}(k)$ fits the tight-binding energy bands *with* OM.

$$\Delta(k) = \underbrace{i\Delta_S \sigma_y}_{\text{s-wave}} + i \underbrace{\mathbf{d}(k) \cdot \boldsymbol{\sigma}}_{\text{p-wave}} \sigma_y$$

Large interfacial SOI → $\mathbf{d}(k) = \Delta_T \mathbf{g}(k)$

$$\text{Gap equation near } T_c \rightarrow [1 - V_S A(T_c)][1 - V_P A(T_c)] = V_S V_P B^2(T_c) \quad B \ll A$$

V_S, V_P attractive potentials for s-, p- wave pairing respectively

→ Topological superconductivity

$$H(k) = \sum (\varepsilon(k) - \mu) c_{k\sigma}^\dagger c_{k\sigma} + \frac{1}{2} \sum \Delta_{\sigma\sigma'}(k) c_{k\sigma}^\dagger c_{-k\sigma'}^\dagger + \frac{1}{2} \sum \Delta_{\sigma'\sigma}^* c_{-k\sigma'} c_{k\sigma} + \alpha \sum \mathbf{g}(k) \cdot \boldsymbol{\sigma}_{\sigma\sigma'} c_{k\sigma}^\dagger c_{k\sigma'}$$

$$\Delta(k) = \underbrace{i\Delta_S \sigma_y}_{\text{s-wave}} + i \underbrace{\mathbf{d}(k) \cdot \boldsymbol{\sigma}}_{\text{p-wave}} \sigma_y$$

Large interfacial SOI → $\mathbf{d}(k) = \Delta_T \mathbf{g}(k)$

$$E(k) = \pm \sqrt{(\varepsilon(k) - \mu)^2 + \Delta_S^2 + \mathbf{g}(k)^2 (\alpha^2 + \Delta_T^2) \pm 2[(\varepsilon(k) - \mu)\alpha + \Delta_S \Delta_T] \|\mathbf{g}(k)\|}$$

→ Gap closing and topological regime if $(\Delta_T \mathbf{g}(k))^2 = (\Delta_S)^2$; $(\varepsilon(k) - \mu)^2 = \alpha^2 \mathbf{g}(k)^2$

BUT!! even when $d_3=0$, we may get a Berry curvature due to the band anisotropy

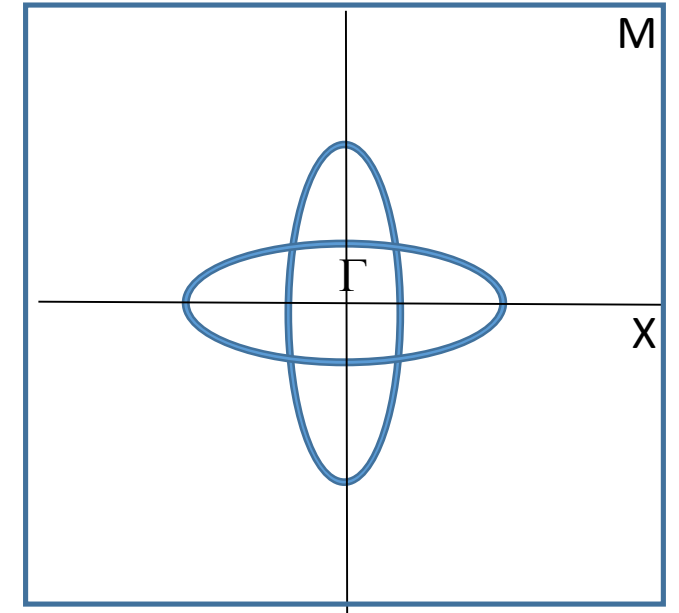
$$H = \begin{pmatrix} ak_x^2 + bk_y^2 & -i\alpha_R k_- \\ i\alpha_R k_+ & bk_x^2 + ak_y^2 \end{pmatrix}$$

$$\varepsilon_0 = \frac{1}{2}(a+b)(k_x^2 + k_y^2) \quad \Delta' = \frac{1}{2}(a-b)(k_x^2 - k_y^2) \rightarrow$$

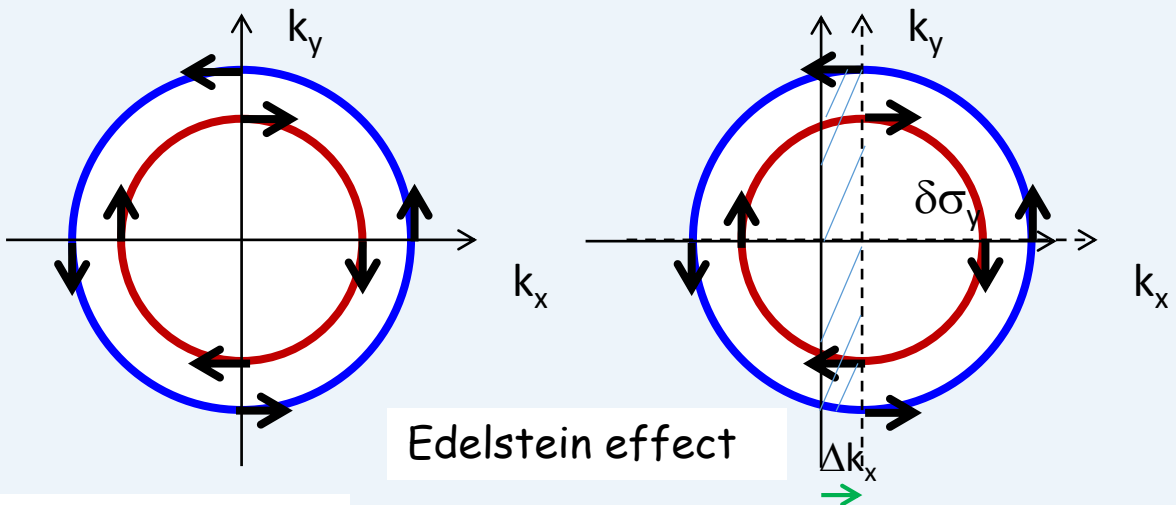
$$H = \varepsilon_0(\mathbf{k})\sigma_0 + \begin{pmatrix} +\Delta' & -i\alpha_R k_- \\ i\alpha_R k_+ & -\Delta' \end{pmatrix} \leftarrow \mathbf{d} \cdot \boldsymbol{\sigma}$$

$$\Omega^z \mp \frac{1}{2} \hat{\mathbf{d}} \cdot (\partial_{k_x} \hat{\mathbf{d}} \times \partial_{k_y} \hat{\mathbf{d}})$$

$$\Omega^z = \mp \frac{1}{2} \alpha_R^2 \frac{\Delta'(\mathbf{k})}{(\Delta'^2 + \alpha_R^2 k^2)^{3/2}}$$



[back](#)

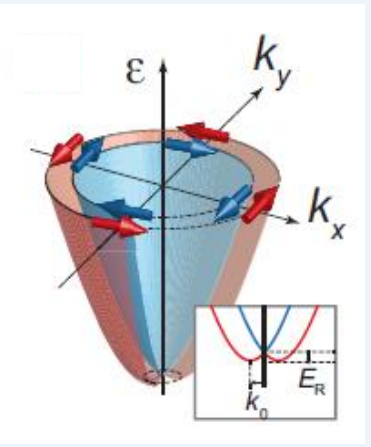


Edelstein effect

$\kappa \equiv$ conversion efficiency of EE (*spin or orbital*)

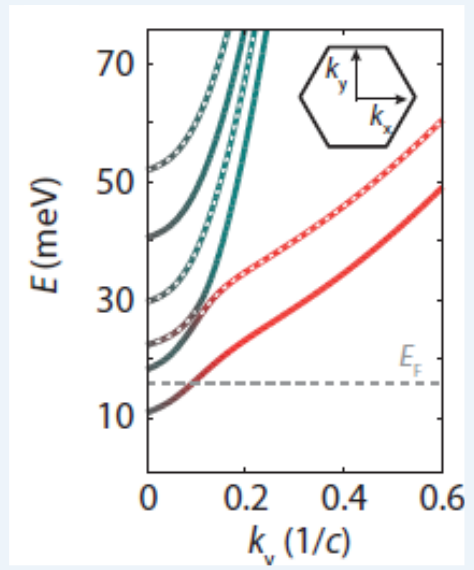
$$\kappa(\mu) = \frac{e\tau_0}{2\pi\hbar} \sum_{\nu} \int_0^{2\pi} d\varphi k_F(\varphi) \langle S \rangle_{\nu}^T(\varphi)$$

$$\kappa(\mu) = \frac{e\tau_0}{2\pi\hbar} \sum_{\nu} \iint_{BZ} d^2k f_{\nu k}(\mu) (\nabla_{\mathbf{k}} \times \langle \vec{S} \rangle_{\nu}) \cdot \vec{z}$$

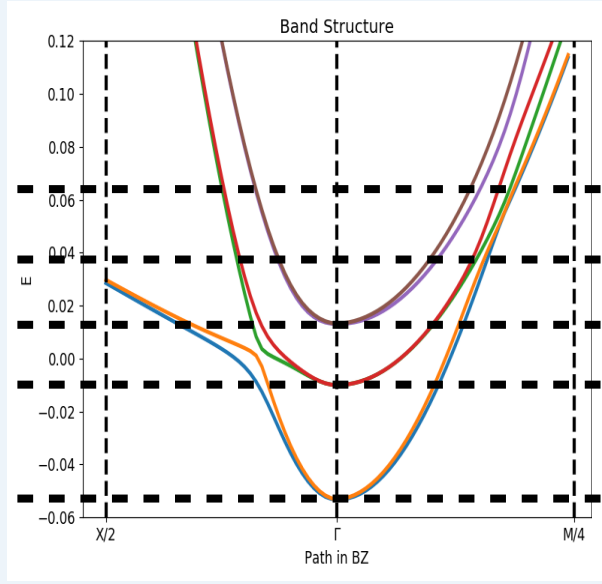


Solid State, Commun. **73**, 233–235 (1990)

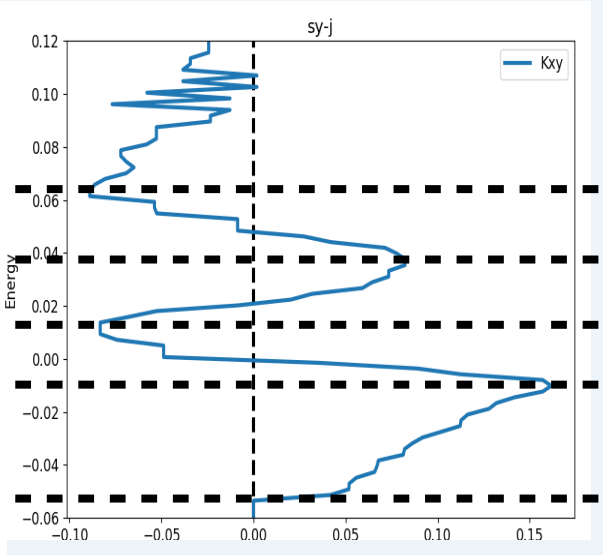
Barnes et al. *Sci. Repts.* **4**, 4105 (2014)



LAO/STO (111)



LAO/STO (001)



Edelstein coefficient

[back](#)